Version of Record: https://www.sciencedirect.com/science/article/pii/S092540052101042X
Manuscript_1af756df91b22169f192d68349e3d39d

Chemiresistor sensor based on ion-imprinted polymer (IIP)-functionalized rGO for Cd(II) ions in water

Jingfang Hu[1,2,3,4*], Mohammed Sedki[5], Yu Shen[2], Ashok Mulchandani[2,6*], Guowei Gao[1,3]

[1]Beijing key Laboratory of sensor, Beijing Information Science & Technology University, Beijing 100101, China

[2]Department of Chemical and Environmental Engineering, University of California, Riverside, CA 92521, United States

[3]Key Laboratory of Modern Measurement and Control Technology, Ministry of Education, Beijing Information Science and Technology University, Beijing 100192, China

[4]State Key Laboratories of Transducer Technology, Shanghai Institute of Microsystems and Information Technology, Chinese Academy of Sciences, Shanghai 200050, China

[5]Material Science and Engineering Program, University of California, Riverside, CA 92521, United States

[6]Center for Environmental Research and Technology (CE-CERT), University of California, Riverside, CA 92507, United States

*Corresponding authors.

E-mail addresses: jfhu@bistu.edu.cn(J. Hu), adani@engr.ucr.edu (A. Mulchandani).

Abstract

This study reports the design and development of a novel chemiresistor (CR) sensor using ion imprinted polymer (IIP)-functionalized reduced graphene oxide (rGO) [IIP/rGO-CR] for cadmium ions (Cd(II)) determination in water. The sensor consisted of a CR transducer made of rGO channel bridging source and drain electrodes prepared by self-assembly and thermal reduction of graphene oxide (GO) on Au interdigitated electrodes chip fabricated on Si/SiO_2 substrate. The IIP was then grafted on rGO using surface-initiated reversible addition-fragmentation chain transfer (RAFT) polymerization with polyethylenimine (PEI) and methylacrylic acid (MAA) as dual functional monomers and Cd(II) ions as template through UV light-initiated copolymerization. The IIP functionalized on rGO acted as an effective recognition element that modulated the resistance of rGO-CR upon binding of Cd(II), enabling Cd(II) detection at ppb level in aqueous solutions. The prepared IIP/rGO-CR sensor worked effectively in the linear range of 2～200 ppb and achieved a limit of detection (LOD) of 0.83 ppb, which is lower than the World Health Organization guidelines of 3 ppb for drinking water quality. The developed sensor of IIP/rGO-CR showed a high selectivity against a variety of trace and heavy metal ions found in water and good stability for up to 60 days when stored at room temperature for Cd(II) determination in water. Further, the sensor was successfully applied to analyzing Cd(II) spiked in tap, lake and river waters with a 94.5% to 113.5% recovery, demonstrating a high degree of accuracy even in complex water samples. Our results illustrated that the CR sensor of IIP functionalized rGO provides a potential platform for sensitive, robust and low-cost environmental analysis of Cd(II) in water.

Keywords: ion imprinted polymer (IIP), rGO, chemiresistor, heavy metals, field-effect transistor (FET)

© 2021 published by Elsevier. This manuscript is made available under the Elsevier user license
https://www.elsevier.com/open-access/userlicense/1.0/

1. Introduction

Chemical and biological sensors based on nanomaterials and field-effect transistor (FET)/chemiresistor (CR) transducers are being actively researched for applications in healthcare and environmental monitoring. These sensors attracted a huge attention due to their high sensitivity, fast response time, real-time measurement capability, low power consumption, potential of miniaturization and portability. In the area of environmental monitoring, sensors for monitoring toxins, pathogens, and heavy metals in water have been reported. The operating principle of a CR/FET sensor is based on the change in electrical resistance that responds to chemical stimuli [1-3]. A CR can be regarded as a FET without applying a physical gate voltage and is therefore easier to operate. The concept of using a CR/FET device for chemical sensing has been demonstrated using a variety of semiconducting materials as channels, such as metal oxides [4], silicon nanowires (SiNWs) [5], carbon nanotubes (CNTs) [6], etc. Of the various semiconducting nanomaterials, reduced graphene oxide (rGO) is gaining a great attention as a channel material in CR/FETs for monitoring of chemical ions such as Na(I), Mg(II), Ca(II), Pb(II) and Hg(II) in water [7-10]. A majority of these sensors used biological materials such as enzymes, DNA, proteins and cells to modify the rGO channel of CR/FET for specific recognition of metal ions to achieve high sensitivity and specificity. However, these biological materials potentially increase the fabrication cost and usually associate with poor stability and reproducibility, which limit their practical application. Therefore, replacing the biological receptors with synthetic recognition materials with high selectivity, excellent chemical and mechanical stability, enhanced shelf life, and low cost is an emerging approach [11,12].

Ion imprinting technology (IIT) is a template-assisted synthesis technology for the production of highly selective imprinted cavities in a 3D-polymeric network [13]. Since the cavities are formed by removing the template metal ions from the polymer matrix, they are highly complementary to the ion template not only in size and shape, but also in the orientation of the functional groups generated in the polymerization process. Thus, the cavities show a “good memory” to the template/target ions. Compared to traditional biological recognition elements, ion-imprinted polymers (IIPs) have further advantages, including ease of preparation, high environmental stability, good reusability and low cost [14]. Thus, IIPs are expected to be promising artificial receptor candidates immobilized on CR/FET transducer channel for specific sensing of target metal ions.

Water contamination with heavy metals is a global concern due to their serious health effects [15]. Cadmium ions (Cd(II)) is one of the highly toxic and non-biodegradable heavy metals that can be transported long distances from emission source in the environment. Ingested cadmium accumulates in the body organs and causes a variety of adverse health effects, especially in kidneys, liver, lung, bone and blood. The International Agency for Research on Cancer (IARC) classified Cd(II) as a human carcinogen at low levels of exposure and is ranked as the seventh most toxic substance to humans by America Toxic and Disease Registry (ATSDR) [16-20]. The European Union regulation limits the Cd(II) at 10 ng/mL (10 ppb) for marine and 5 ppb for fresh water [21]. The World Health Organization (WHO) recommends a 3 ng/mL (3 ppb) maximum concentration limit for Cd(II) in drinking water [22]. Therefore, the detection of trace cadmium in water is essential for the management of water pollution.

In this work we report, for the first time, a Cd(II) sensor based on IIP-grafted rGO-CR/FET.

The rGO-CR/FET was prepared by self–assembly followed by thermal reduction. Then, the IIP was synthesized on the rGO film using surface-initiated reversible addition-fragmentation chain transfer (RAFT) polymerization method, which was recently demonstrated as an improved strategy to prepare IIPs with controlled thickness, homogeneous distribution of imprinted sites and terminal functionality [23]. Unlike conventional imprinting polymerization, RAFT polymerization enables the tethered polymer chains to form and grow on the surface and propagates outward into the solution. For improving the specific binding strength to the target ion Cd(II), dual functional monomers of polyethylenimine (PEI) and methylacrylic acid (MAA) were implemented, through UV light-initiated copolymerization, to provide a synergic effect for immobilization of template ion Cd(II) on rGO film. Subsequently, the performance of the developed chemiresistor sensor were characterized and discussed for the analysis of Cd(II) detection in water. We achieved an ultralow detection limit of 0.83 ppb, with superior selectivity of Cd(II) against interfering ions. Furthermore, high recovery/accuracy was demonstrated with natural water samples spiked with Cd(II).

2. Experimental

2.1 Materials

GO was synthesized using improved Hummer method, with some modifications, as reported earlier [24]. 1-Pyrenemethanol,3-chloropropyltrimethoxysilane, cadmium acetate, methacrylic acid (MAA), polyethylenimine (PEI, MW 600), sodium N,N-diethyldithiocarbamate trihydrate and ethylene glycol dimethacrylate (EGDMA) were obtained from the Sigma Aldrich (St. Louis, MO, USA). Dimethyl formamide (DMF), dimethyl sulfoxide (DMSO), (3-aminopropyl)triethoxysilane (ATPES), hydrochloric acid (HCl), toluene, acetone, ethanol and other metal ion salts such as $AgNO_3$, $CuCl_2$, $Hg(NO_3)_2$, $NiCl_2$, $Pb(NO_3)_2$, $Pd(NO_3)_2$, $Zn(NO_3)_2$ were purchased from Fisher Scientific (Chino, CA, USA). All solutions used in the experiments were prepared with ultrapure water from a Milli-R04 purification system (Millipore, Burlington, MA, USA).

2.2 Fabrication of rGO-FET device

Fig S1(A) (shown in the supplementary information) illustrates the schematic of the fabrication process of the IIP/rGO-CR/FET sensing device. The process consisted of 1) microfabrication of chips consisting of 5 interdigitated electrodes (IDE) per chip (as shown in Fig. S1(B)) that were patterned on an Si/SiO_2 substrate (300 nm thick SiO_2 layer) by photolithography, followed by the deposition of a 5 nm Cr layer and a 50 nm Au layer by e-beam evaporation. 2) The cleaning of diced chip sequentially with acetone, ethanol and deionized water and dried with N_2. 3) The self-assembly of GO. 4) Thermal reduction of GO to rGO. 5) Modification of rGO with IIP by RAFT. The self-assembly of GO on the patterned IDE for the preparation of rGO-FET is shown in Fig. S2 (shown in the supplementary information). The process consisted of four steps. 1) Incubation of electrodes with ammonium hydroxide (30% v/v) solution for 30 min to introduce –OH groups and washing with deionized water to remove additives on the chip. 2) Incubation with APTES for 2 h and washing with deionized water. 3) Drop casting of 10 µL of 1.25 mg/ml GO suspension followed by drying for 2 h at room temperature to self-assemble GO on the gate channel through –COOH and $–NH_2$ electrostatic interactions. 4) Heating GO-FET chip at 200℃ for 2 h to reduce GO to rGO. The fabricated rGO-FET were kept in vacuum drying chamber for

further use.

2.3 Preparation of IIP on the rGO-CR/FET

The rGO-CR/FET was functionalized with IIP by surface RAFT polymerization using the method reported previously [25]. In this study, MAA and PEI, forming anion and cation, were used as the dual functional monomers to form a complex with the target ions of cadmium. In fact, PEI could be used not only as a chelator for the cadmium metal cations in a neutral solution, but also as a proton acceptor for the MAA, which could assist better dissociation of carboxyl group and improve the binding strength of the carboxylate to cationic cadmium ions [26]. Fig. 1a illustrates the IIP preparation procedure. In brief, the rGO-FET chip was first immersed into 6 mM 1-pyrenemethanol (1-Pym) solution for 3 h and the resultant rGO-OH was washed with water to remove excess 1-Pym from the chip surface. Subsequently, the chip was soaked into 0.5 μM 3-chloropropyltrimethoxysilane in 10 mL toluene and heated at 80℃ for 4 h to introduce 3-chloropropyl groups on rGO surface. After washing with water, the chip was dipped in 10 mL ethanol containing 3 mM sodium N,N-diethyldithiocarbamate trihydrate and incubated for 12 h at room temperature to graft the photoactive iniferter on the rGO surface. Then cadmium acetate (0.2 mM) was dissolved in 5 ml of DMSO containing 0.3 mM MAA and 0.15 mM PEI as functional monomers for 1 h to obtain a prepolymer solution (the optimization of the concentration ratio of MAA and PEI is shown in Fig. S3). Next, 2 mM ethylene glycol dimethacrylate (EGDMA) as cross-linker, and 1 mg azodiisobutyronitrile (AIBN) as initiator were added in the prepolymer solution and flushed with nitrogen gas to remove oxygen to prevent oxygen from reacting with the free radical. 10 μL of the prepared solution were added on the surface of the photoactive iniferter-grafted rGO-CR/FET chip and exposed to UV light (λ =254 nm) for 12 h, resulting in the formation of IIPs on rGO surface. After UV polymerization, the resulting sensor chip was washed several times with hydrochloric acid solution (0.1 M) and ethanol to remove the Cd(II) template from the polymer matrix and residual unreacted solvent, respectively. The conceptual structure of the proposed sensor chip is shown in Fig. 1b, and the RAFT polymerized IIP on rGO is illustrated in Fig. 1c. For comparison, the no-template imprinted polymer (NIP) was also prepared using the same procedure but without the addition of Cd(II) template.

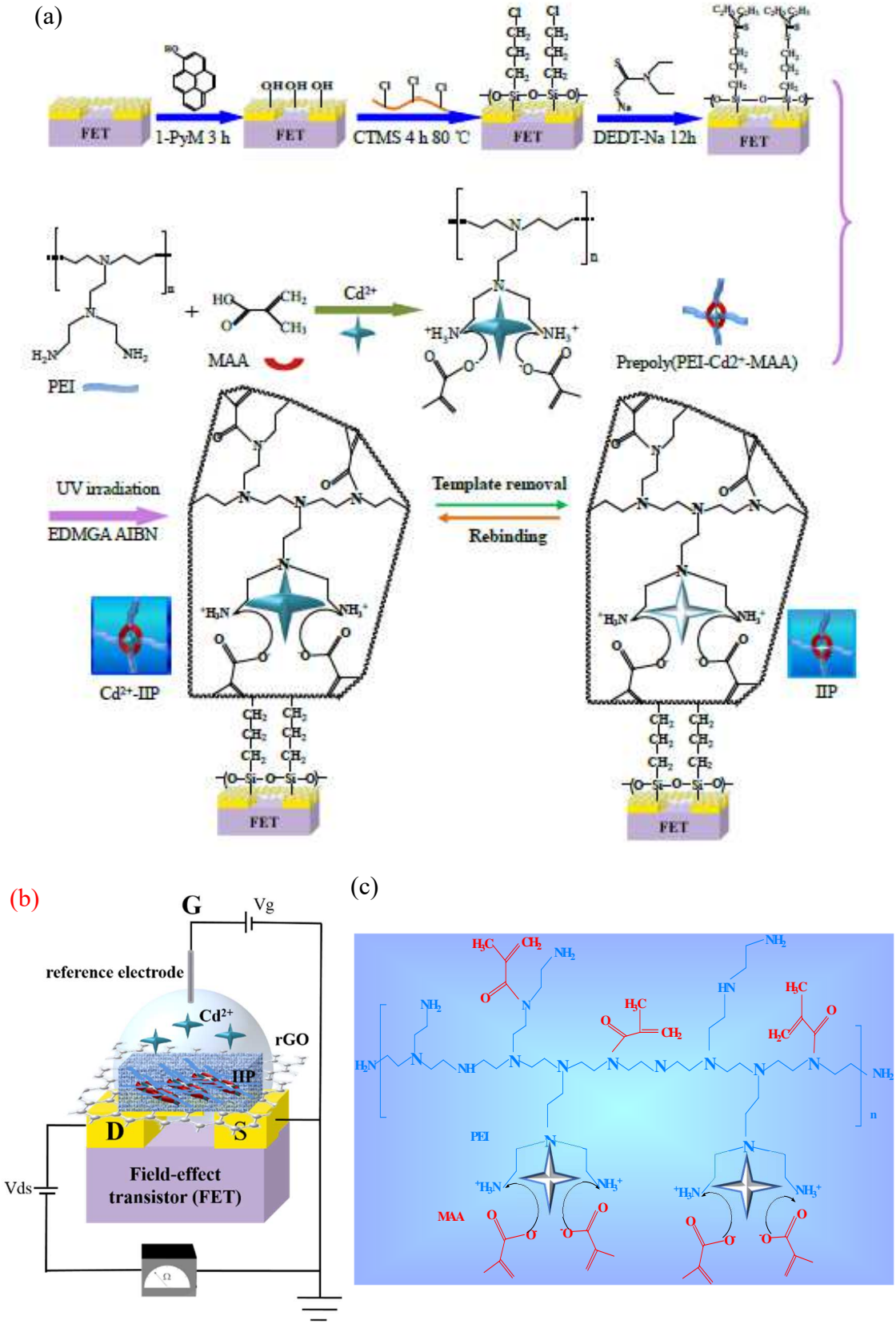

Fig. 1. Illustration of surface RAFT polymerization, CR/FET sensor, and the chemical structure of IIP. (a) Schematic of surface RAFT polymerization protocol for immobilization of IIP on rGO-CR/FET. (b) Schematic of the IIP/rGO-CR/FET sensor for Cd(II) sensing. (c) Chemical structure of the RAFT polymerized IIP on rGO.

2.4 Characterization

The surface morphology of the self-assembled rGO and RAFT polymerized IIP were examined using scanning electron microscopy (SEM) (TESCAN Vega3 SBH). Polymerization and Cd(II) binding/removal were analyzed using Fourier transform infrared spectrometer (FTIR, Thermo Nicolet 6700). The electrical current-voltage (I_{ds}-V_{ds}) and transfer curve characteristics (I_{ds}-V_g) characterization of the fabricated sensors were performed using Keithley 2636B source meter and measurement unit (Tektronix Inc., Beaverton, OR, USA). The transfer curve (I_{ds}-V_g) characterization was conducted by liquid-ion gating in a 100 µL blank solution (acetic acid/sodium acetate/sodium hydroxide pH 7.0) with Ag/AgCl reference electrode.

2.5 Sensing procedure

The electrical measurement was carried out with a Keithley source meter at room temperature. A 200 µL volume PDMS chamber was attached onto the IIP/rGO-CR/FET sensing channel. A 100 µL blank solution was pipetted into the chamber and the sensing channels were incubated until the resistances in the channels were stable, followed by additions of 10 µL Cd(II) spiked samples prepared in the blank solution. Each time, 10 µL of the Cd(II) analyte sample were pipetted onto the CR/FET sensing channel, and the source-drain current (I_{ds}) versus source-drain voltage (V_{ds}) at V_g at 0 V were recorded after 5 min incubation. Following each measurement, the sensing channel as washed with 0.1 M hydrochloric acid and water and dried with nitrogen gas.

2.6 Real samples analysis

Water samples analysis included tap water (pH 6.7), lake water (pH 8.3) and river water (pH 7.8) collected from Beijing city, China. Prior to analysis, water samples were filtered with 0.22 µm membrane to remove large particles and analyzed for Cd(II) by the traditional method of inductively coupled plasma mass spectrometry (ICP-MS) (HJ 700-2014, National Environment Protection Standard of China). Water samples were then spiked with Cd(II) ions standard solution to prepare water samples containing 2, 10 and 50 ppb Cd(II). The pH of the solutions was fixed at 7.0. 10 µL of spiked samples were added into the blank solution for measurements. To quantify Cd(II) ions concentration in the real samples, a calibration curve between $(R\text{-}R_0)/R_0$ [where, R_0 and R, respectively, are the IIP/rGO-CR sensor resistance before and after incubation with Cd(II) sample] versus Cd(II) concentration was obtained, and then the samples were analyzed by the sensor with the same procedure as above.

3 Results and discussion

3.1 Characterization of rGO and IIP

Fig. 2(A) shows the SEM micrograph of rGO layer on the IDE array; typical wrinkled structures (Fig. 2(B)), indicate the successful self-assembly of rGO sheets on the CR/FET channel. After the IIP layer was grafted on rGO sheets, showed in Fig. 2(C), a rough surface can be observed in the SEM image in Fig. 2(D), suggesting that a solid polymer film was successfully formed using RAFT polymerization method. For comparison, the morphological characterization of NIP (imprinted polymer without Cd(II)) and IIP, respectively, were further assessed before template removal (Fig. 2(E) and 2(F)) and after template removal (Fig. 2(G) and 2(H)). As shown in Fig. 2E and Fig. 2F, both of NIP and IIP were smooth before template removal, and no obvious

difference appeared between NIP and IIP. On the other hand, after template removal wash, while the NIP was still smooth (Fig. 2(G)), IIP displayed many nanopores on the polymer surface (Fig. 2(H), original SEM image showed in Fig. S4). This is ascribed to a large number of functional monomers that can center around the cadmium ions template to provide sufficient binding sites, and the template cadmium ions were imprinted into the polymer matrix during UV irradiation. After template removal from the polymer, the nanopores could be formed on the polymer surface, and the open porous structure would allow target ion binding [27, 28]. Therefore, the IIP with specific cavities for Cd(II) binding was successfully grafted on the rGO surface.

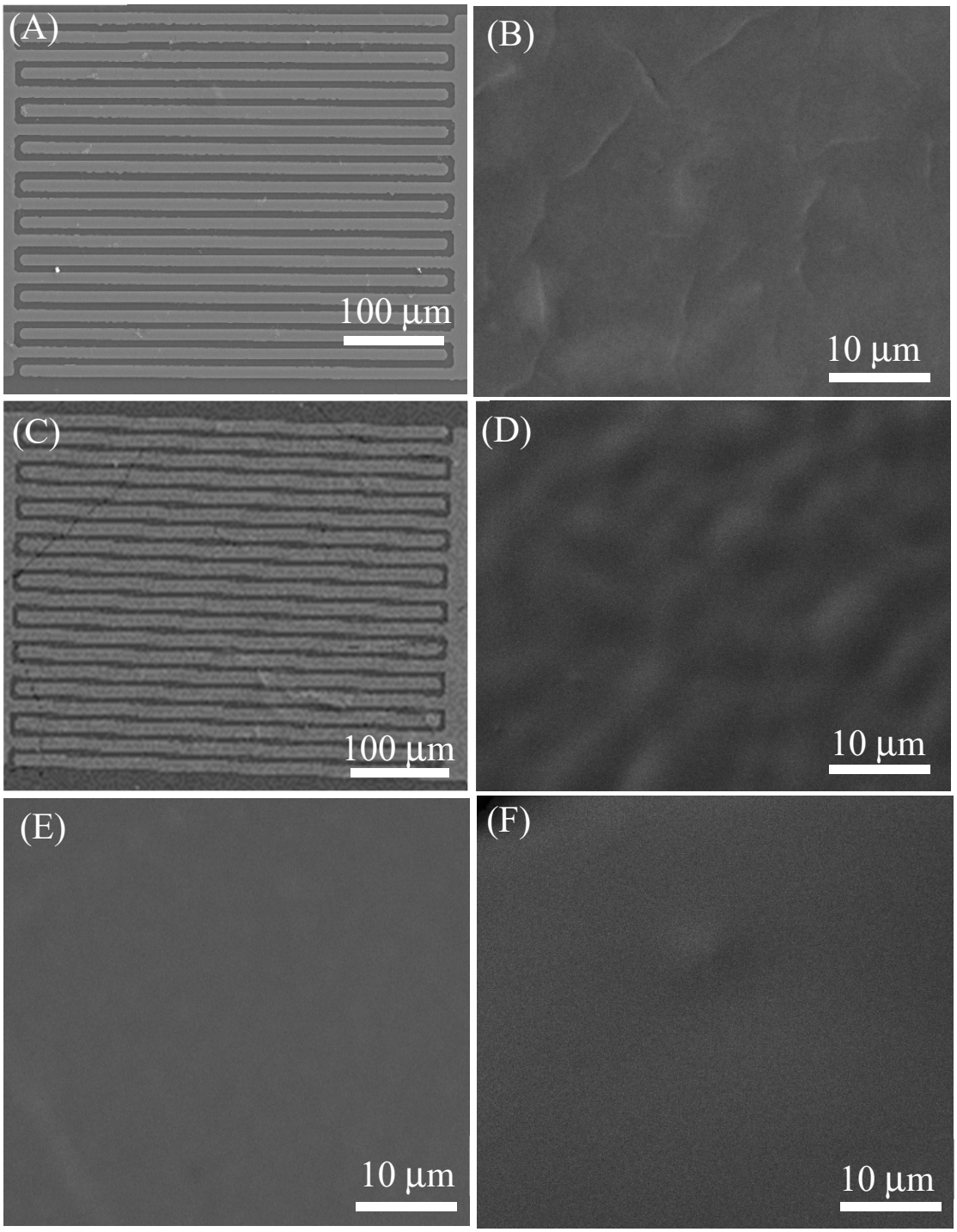

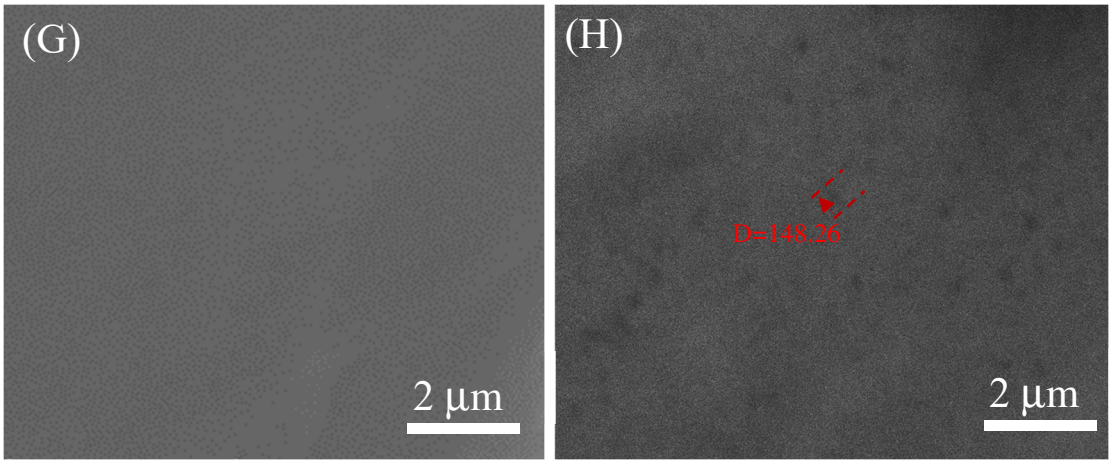

Fig.2. Morphological characterization of rGO, rGO-NIP and rGO-IIP on IDE. SEM micrographs of: (A) rGO film on IDE; (B) partially magnified image of (A); (C) IIP immobilized on rGO-FET; (D) partially magnified image of: (E) NIP without template removal wash; (F) IIP without template removal wash; (G) NIP after template removal wash; and (H) IIP after template removal wash.

Fig. 3 shows FTIR spectra of prepared GO and rGO. In GO sample, there were stretching vibrational peaks of hydroxyl groups at 3400 cm^{-1}, carbonyl groups at 1722 cm^{-1} and C=C at 1627 cm^{-1}. Furthermore, the data show a strong reduction of oxygen functionalities, with the removal of nearly all hydroxyl and most carbonyl groups after 120 min annealing. These results are in a good agreement with literature [29]. As shown in the XRD diffractograms in Fig. 4, GO nanosheets showed a strong and sharp diffraction peak at 2Θ of 9.5° with no graphite peak at 26°, which confirms the complete oxidation of graphite flakes into GO. On the other hand, reducing GO results in stripping the oxygen functionalities, that were pushing the sheets apart, and hence reduces the spacing between the rGO nanosheets and shifts the diffraction peaks into higher 2Θ values. In this regard, the thermal reduction of GO sample at 200°C and ambient air conditions for a 120 min exhibited a diffraction peak at 23.80°, confirming the high reduction level of GO nanosheets. Results are matching the conclusions of above FTIR results and published literature [30]. It is worth mentioning that at 120 min reduction, the diffraction peak of GO was completely diminished, which validates the homogenous reduction of GO nanosheets.

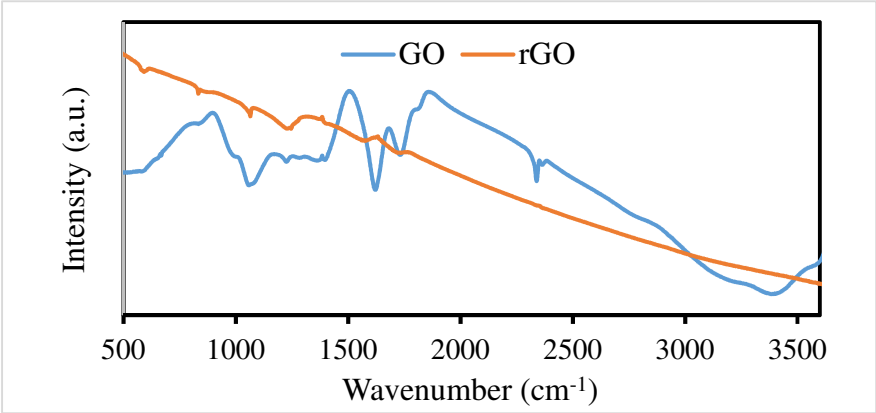

Fig. 3. FTIR analysis of GO and rGO nanosheets

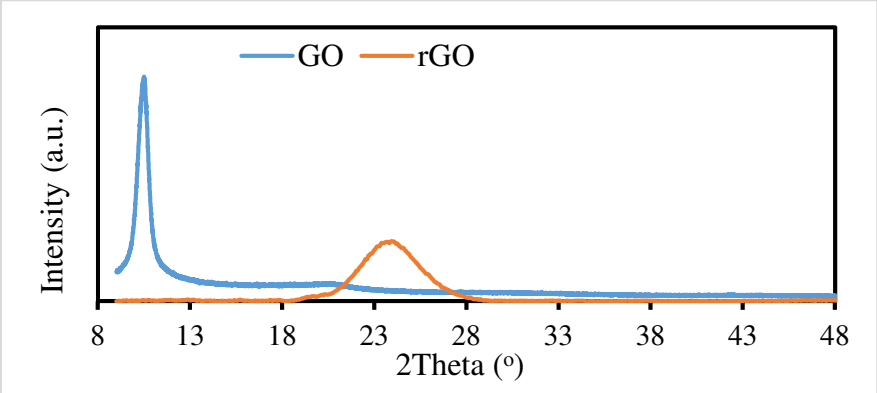

Fig. 4. XRD analysis of GO and rGO nanosheets

In further, the polymers of NIP, Cd(II)-IIP (before template removal wash) and IIP (after template removal wash) were examined by FTIR. As shown in Fig. 5, all the FTIR spectra had a broad band at 3300-3500 cm^{-1}, which was attributed to the stretching vibration of N-H in functional monomer PEI and O-H stretching from the intramolecular and intermolecular hydrogen bonds. The vibrational bands at 2700-3000 cm^{-1} were assigned to the C-H stretching from alkyl groups. The C-N stretching vibration of secondary amine appeared at 1298 cm^{-1} and the N-H bending of secondary amine appeared at 1458 cm^{-1}, which confirmed the reaction between PEI and MAA. The C=O stretching vibration of the amide group was observed at 1650 cm^{-1} in the NIP and the unremoved IIP, and shifted to 1729 cm^{-1} in removed IIP, showing the involvement of the oxygen of C=O group in the cadmium reaction [31]. A typical peak at 952 cm^{-1} was observed only in unremoved IIP reaction, which can be attributed to the stretching vibration of Cd-O, indicating that an ionic complex may be established between MAA and cadmium ions via ionic interactions [32]. In addition, the decrease in the intensity of these absorption bands in the unremoved IIP was the result of their interaction with cadmium ions. Therefore, the FTIR characterization further suggested that the IIP was successfully coated on rGO-CR/FET.

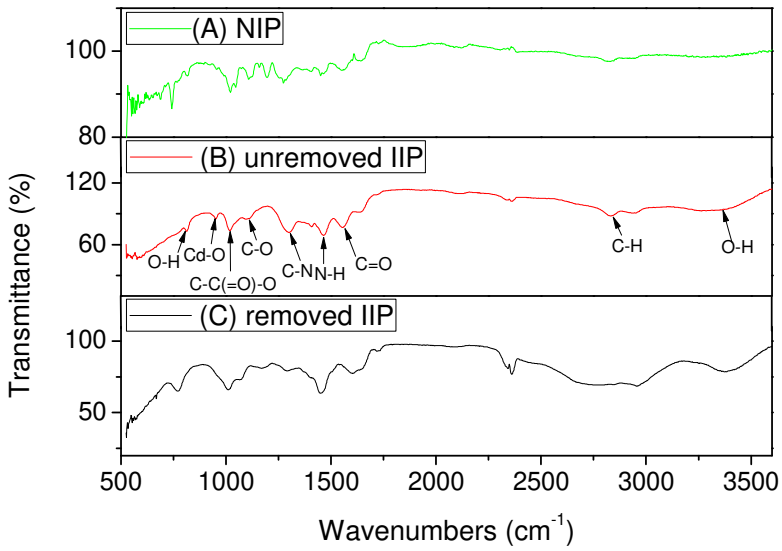

Fig. 5. FTIR spectra of NIP (A), unremoved IIP (B), and removed IIP (C)

3.2 Electrical characterization of IIP modified rGO-FET

For the FET sensor, the source-drain current-voltage (I_{ds}-V_{ds}) and transfer curve characteristics (I_{ds}-V_g) of the semiconductor channel are critical to the sensing performance. First, the rGO-FET without IIP was tested to check the effect of modification by IIP. A typical transfer curve, with the ambipolar behavior of pristine graphene, was obtained with a Dirac point near 0 V (shown in Fig. S5(A)), which suggested that the prepared rGO has a negligible number of defects (impurities doping) [33]. The I_{ds}-V_{ds} characteristic of the rGO-FET was also measured with V_g varying from -0.2 V to 0.2 V (shown in Fig. S5(B)). It can be found that I_{ds} decreased as V_g increased from -0.2 V to 0 V, but increased as V_g increased from 0 V to 0.2 V, which showed that carriers of electrons are nearly equal to the carriers of holes in rGO sheets after the thermal reduction process. However, after IIP modification on rGO-FET, it was observed that the transfer curve shifted to the positive side, as shown in Fig. 6. It shows not only a shift of the Dirac point, but also a decrease of the overall current level due to the polymer modification. The possible reason is doping of rGO from the residue and the IIP changing the main charge carrier in the rGO surface to holes, resulting in a p-type semiconductor and a decreased source-drain output current after IIP modification.

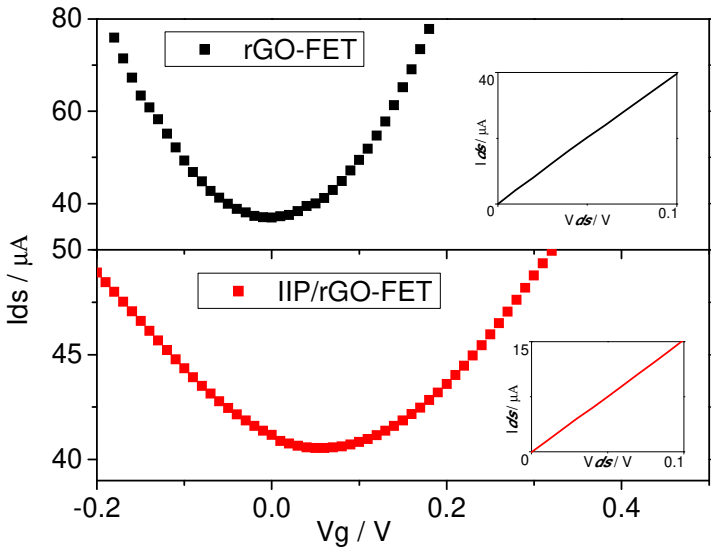

Fig. 6. Transfer curves of liquid-ion gating rGO-FET (top) and IIP/rGO-FET (bottom) with 0.1 V source-drain voltage. Insets: I_{ds}-V_{ds} curves of rGO-FET and IIP/rGO-FET at Vg of 0 V.

As shown in Fig. 6 (insets), the I_{ds}-V_{ds} curves at V_g = 0 V of both rGO-FET and IIP/rGO-FET were linear, suggesting there was an Ohmic contact between the gold IDE and rGO as well as the IIP/rGO. Therefore, responses of the rGO-FET, IIP/rGO-FET and NIP/rGO-FET to Cd(II) were investigated by recording their resistances in different Cd(II) concentrations at zero gate, i.e. in chemiresistor mode. As a first step, to assess the benefit of IIP as recognition element in Cd(II) detection, we compared the responses, the normalized chemiresistive resistance change

($\Delta R/R_0$) (where, R_0 is the resistance before Cd(II) addition and ΔR is difference between the resistance after Cd(II) addition and before Cd(II) addition), of rGO-CR, NIP/rGO-CR and IIP/rGO-CR (the former two served as controls) to 5, 100, 250 and 500 ppb Cd(II). The results, as shown in Fig. 5, clearly demonstrated the significant benefit of the IIP on the rGO-CR response to Cd(II), confirming the significant contribution of Cd(II) binding sites in IIP.

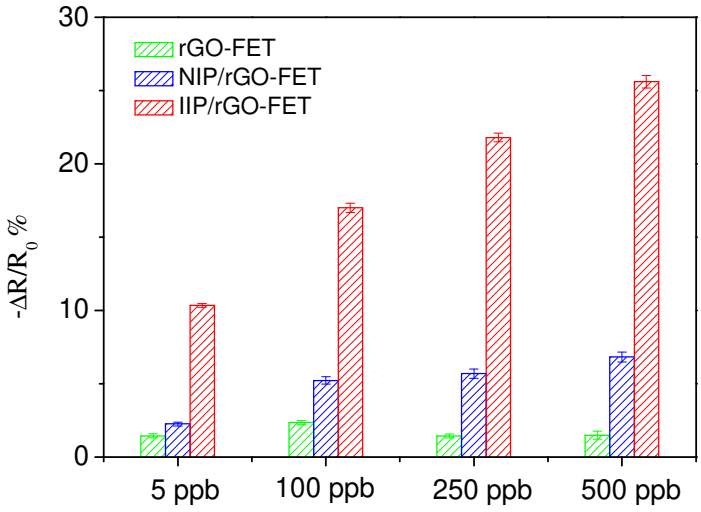

Fig. 7. Normalized resistance changes of rGO-CR, NIP/rGO-CR and IIP/rGO-CR as a function of Cd(II) concentrations at pH 5.0. The error bar represents ±1 standard deviation from 3 successive measurements.

For a better understanding of the sensing mechanism, we investigated the effect of Cd(II) ion concentrations on transfer curve characteristics of the IIP/rGO-FET. It was found that the transfer curves shifted toward positive direction with increasing Cd(II) ion concentration, which can be explained by the increased p-doping of IIP/rGO-FET from the adsorption/binding of increasing amounts of Cd(II) in IIP (for more information please see Fig. S5). Furthermore, the slope of the FET curve on the right side, where the positive gate voltage is applied (at 200 ppb), decreased due to the depletion of part of the electron carriers in the material due to the p-type doping of IIP-rGO caused by Cd(II). The positive shift of Dirac point is in concurrence with the resistance decrease observed previously in Fig.7.

3.3 Effect of pH on Cd(II) sensing with IIP/rGO-CR

Fig. 8 shows the effect of pH on the response of IIP/rGO-CR sensor for detection of 50 ppb Cd(II) in solution. The sensor responses were determined in the pH range 2.0～10.0 and pH adjustment in the solutions were made with diluted hydrochloric acid or sodium hydroxide. The results show a sharp increase in the sensor response from a low value of 0.9 % at pH 2 to a maximum response of 17.5% at pH 7.0 followed by a decline to 13.5% at pH 9. The observed trend can be attributed to the weak binding reaction between Cd(II) and active atoms in imprinted sites at low pH values due to the protonation of IIP active sites and precipitation of

$Cd(OH)_2$ at pH above 9.0. Based on this, pH 5.0～9.0 could be the sensor working range, and pH 7.0 was used in subsequent analytical characterization of IIP/rGO-CR sensor.

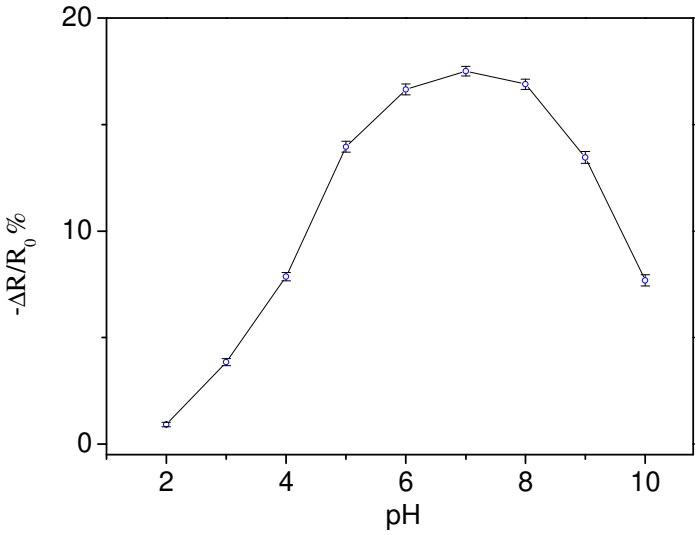

Fig. 8. Effect of pH on the $\Delta R/R_0$ responses to 50 ppb Cd(II) solution. The error bar represents ±1 standard deviation from 3 successive measurements.

3.4 Cd(II) sensing with the IIP/rGO-CR

We evaluated the performance of IIP/rGO-CR sensor in terms of sensitivity, limit of detection, selectivity and stability. As shown in Fig. 9, there was a good linearity of resistance change *vs* Cd(II) concentration from 2 ppb to 200 ppb with a sensitivity (slope of the plot) of 0.14 ppb^{-1}. The limit of detection, calculated based on S/N = 3, was estimated to be 0.83 ppb, which was well below the guideline value of Cd(II) in drinking water (3 ppb) set by WHO.

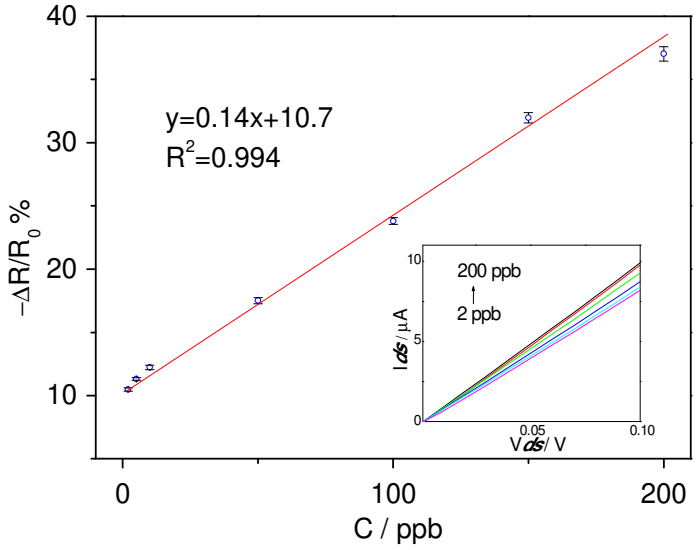

Fig. 9. Response of IIP/rGO-CR sensor as a function of Cd(II) concentration at pH 7.0. The inset is I_{ds}-V_{ds} curves of different Cd(II) concentrations from 2 ppb to 200 ppb. The error bar represents ±1 standard deviation from 3 successive measurements.

The selectivity of detection is always a challenging work in sensor development. Hence, the selectivity of the prepared IIP/rGO-CR toward Cd(II) was evaluated by recording the chemiresistive response in the presence of other common heavy metal ions found in water at 100-fold higher concentration (1000 ppb) than Cd(II) in water samples (Fig. 10). As illustrated in the figure, there was an insignificant change/off-set (-2.3% to 7.1%) of the response to even 1000-fold excess of these ions, demonstrating excellent selectivity of the IIP/rGO-CR sensor for Cd(II) against other commonly found trace and heavy metal ions. This excellent selectivity is ascribed to the specific recognition sites complementary to the coordination geometry, coordination number, charge and size of the cavities for Cd(II) in the RAFT imprinted poly(PEI-MAA) film that has a high binding selectivity to Cd(II) than other trace and heavy metal ions.

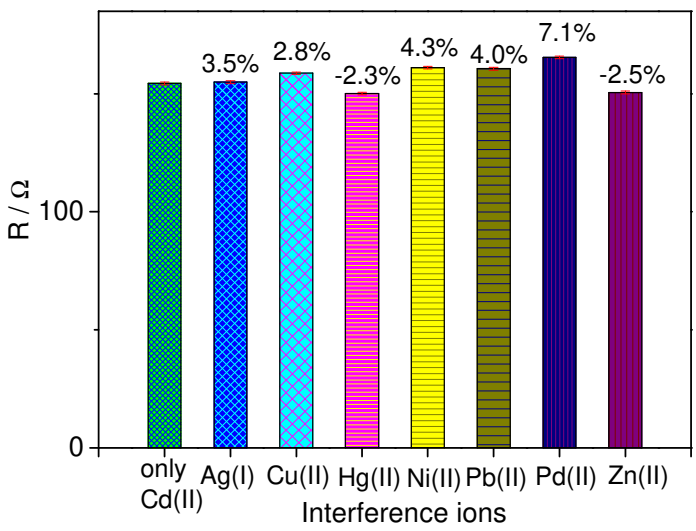

Fig. 10. The resistance offset of IIP/ rGO-CR toward Cd(II) in the presence of 100-fold concentration of Ag(I), Cu(II), Hg(II), Ni(II), Pb(II), Pd(II) and Zn(II). The error bar represents ±1 standard deviation from 3 successive measurements.

Another important factor of the sensors is the stability. The long-term stability of the proposed IIP/rGO-CR was investigated by measuring the response to 10 ppb of Cd(II) standard solution every 5 days for 2 months (60 days) period. As shown in Fig. S7, no observable change in the resistance response was observed after the sensor was stored for the first 5 days at room temperature in vacuum. The resistance response of the chemiresistor sensor only decreased to 93% after storing for 30 days, and still retained above 85% of the original response after 60 days. The high long-term stability of the imprinted films can be credited to the *in situ* RAFT polymerized IIP recognition element at the rGO-FET surface.

Table 1 presents a comparison of some important characteristics of the proposed sensor with the corresponding values for previously reported Cd(II) electrochemical/electrical sensors based

on different sensing materials. It can be found that the sensing performance of our CR sensor is comparable or superior to other reported sensors for Cd(II) determination by showing its high sensitivity, low LOD, and wide dynamic range. In particular, the proposed CR sensor of IIP/rGO-CR can be potentially used in neutral water environment that is advantageous for direct application in natural water samples.

The above results clearly demonstrated the benefits of combining the unique properties of the Cd(II)-imprinted poly(PEI+MAA) with rGO-CR in highly sensitive, selective, and cost-effective Cd(II) monitoring in water.

Table 1. Comparison of our proposed method to other different methods for Cd(II) determination

Method[a]	Sensing material[b]	Linear range(ppb)	LOD (ppb)	pH	Stability	Ref.
CR	MPTES/SiNWs	11.2～1120	---	4	24 h	[34]
CR	L-Cysteine/MoS_2	1～500	---	6～7	20 times	[35]
SWASV	G/PANI/PS/SPEC	10～500	4.43	1.0	10 times	[36]
SWASV	HP-β-CD-RGO/Nafion/GCE	0.056～1.008	0.0075	4.5	10 times	[37]
DPASV	IIP-NPs/CPE	0.5～40	0.15	5.0	28 days	[38]
SPR	IIP AuNPs	0.1～50	0.01	4.5	---	[39]
SERS	flower-like Ag@CuO	11.2～11200	2.912	---	---	[40]
CR	IIP/rGO	2～200	0.83	7.0	60 days	This work

[a] CR: chemiresistor; SWASV: square wave anodic stripping voltammetry; DPASV: deferential pulse anodic stripping differential pulse voltammetry; SPR: surface plasmon resonance; SERS: surface-enhanced Raman scattering.

[b] MPTES/SiNWs: 3-mercaptopropyltriethoxysilane/silicon nanowires; G/PANI/PS/SPEC: graphene/polyaniline/polystyrene nanoporous fibers/screen printed carbon electrode; HP-β-CD-RGO/Nafion/GCE: hydroxypropyl-β-cyclodextrin decorated reduced GO/Nafion/glassy carbon electrode; IIP-NPs/CPE: ion imprinted poly(3-[2-(2-aminoethylamino)ethylamino]propyl-trimethoxysilane) nanoparticles/carbon paste electrode; IIP AuNPs: ion imprinted poly(N-methacryloyl-L-cysteine) on gold nanoparticles; IIP/rGO: ion imprinted poly(MAA+PEI)/reduced GO.

3.5 Application for real water samples

To evaluate the practical applicability, the proposed IIP/rGO-CR sensor was used to measure Cd(II) concentration in tap , lake and river waters. The initial measurement by the classical ICP-MS method showed no Cd(II) could be detected in the samples. In this case, Cd(II) standard solution was spiked in the water samples with final concentrations of 2 ppb, 10 ppb, and 50 ppb and then analyzed with the sensor to evaluate the recovery. The results (Table 2) showed that the recoveries of Cd(II) ranged from 94.5% to 113.5% and the relative standard deviation (RSD) ranged from 3.2% to 17.9% . This indicates that the developed sensor has the competence for real water application.

Table 2. Analysis of real water samples spiked with Cd(II) by the IIP/rGO-FET sensor.

Samples	Spiked (ppb)	Determined (ppb)	Recovery (%)	RSD (%)	ICP-MS
Tap water	2	2.12	106	17.53	1.9
	10	10.73	107.3	4.44	10.38
	50	49.56	99.1	6.49	49.86
Lake water	2	2.27	113.5	15.8	2.15
	10	10.86	108.6	6.73	10.42
	50	51.37	102.7	3.2	50.56
River water	2	1.93	96.5	17.9	2.05
	10	9.45	94.5	7.84	10.13
	50	51.53	103	3.42	49.87

4. Conclusions

In summary, we fabricated a CR/FET sensor based on IIP *in situ* grafted on rGO as sensing channel for highly sensitive and specific detection of Cd(II) in water. SEM imaging confirmed the successful imprinting process as shown by the pores formation after washing the analyte out. FTIR spectroscopy verified the successful polymerization on rGO and the binding and washing of the analyte, i.e., the successful imprinting process. The selective binding interaction of Cd(II) with the IIP of Cd(II)-ion imprinted poly(PEI+MAA) on the surface of rGO caused significant change in the resistance of the rGO-FET device, which enabled the detection of Cd(II) at sub-ppb level. Moreover, the proposed sensor showed excellent selectivity toward Cd(II) over other common trace/heavy metal ions, excellent storage stability and highly accurate detection of spiked Cd(II) in real water samples. The simple structure of the chemiresistive sensor combined with IIP functionalization approach renders our sensor an ideal candidate for developing on-site, rapid, and low-cost monitoring tools in real application.

Acknowledgements

We acknowledge financial supports from the US Department of Energy (award number FE0030456) and W. Ruel Johnson Chair in Environmental Engineering to AM and National Natural Science Foundation of China (No. 61601037, No. 61701475) and Development and Improvement of Scientific Research Level Program of Beijing Information and Science University (No. 2019KYNH222) to JH.

References

[1] E. Hoque, L. H. H. Hsu, A. Aryasomayajula, Pencil-Drawn chemiresistive sensor for free chlorine in water, IEEE Sensors Letters, 1 (2017):1-4.

[2] Y. Jiang, N. Tang, C. Zhou, Z. Han, H. Qu, X. Duan, A chemiresistive sensor array from conductive polymer nanowires fabricated by nanoscale soft lithography, Nanoscale, 10 (2018):20578-20586.

[3] A. Mohtasebi, P. Kruse, Chemical sensors based on surface charge transfer, Physical Sciences Reviews, 3 (2018): 20170133.

[4] E. N. Carmona, V. Sberveglieri, A. Ponzoni, V. Galstyan, D. Zappa, A. Pulvirenti, E. Comini, Detection of food and skin pathogen microbiota by means of an electronic nose based on metal oxide chemiresistors. Sensors & Actuators B: Chemical, 238 (2017):1224-1230.

[5] B. Borgne, L. Pichon, A. C. Salaun, B. L. Bihan, A. Jolivet-Gougeon, S. Martin, R. Rogel, O. Sagazan, Bacteria electrical detection using 3D silicon nanowires based resistor, Sensors and Actuators B: Chemical,273 (2018): 1794-1799.

[6] Y. Shen, T. Tran, S. Modha, H. Tsutsui, A. Mulchandani, A Paper-based chemiresistive biosensor employing single-walled carbon nanotubes for low-cost, point-of-care detection, Biosensors & Bioelectronics, 130 (2019): 367-373.

[7] F. Tan, L. Cong, X. Jiang, Y. Wang, X. Quan, J. Chen, A. Mulchandani, Highly sensitive detection of Cr(VI) by reduced graphene oxide chemiresistor and 1,4-dithiothreitol functionalized Au nanoparticles, Sensors and Actuators B: Chemical, 247 (2017):265-272.

[8] F. Tan, L. Cong, N. M. Saucedo, J. Gao, X. Li, A. Mulchandani, An electrochemically reduced graphene oxide chemiresistive sensor for sensitive detection of Hg^{2+} ion in water samples, Journal of Hazardous Materials, 320 (2016):226-233.

[9] H. G. Sudibya, Q. He, H. Zhang, P. Chen, Electrical detection of metal ions using field-effect transistors based on micropatterned reduced graphene oxide films, ACS Nano, 5 (2011):1990-1994.

[10] J. Chang, G. Zhou, E. Christensen, H. Robert, J. Chen, Graphene-based sensors for detection of heavy metals in water: a review, Analytical and Bioanalytical Chemistry, 406 (2014):3957-3975.

[11] Y. Liu, Y. Deng, H. Dong, K. Liu, N. He, Progress on sensors based on nanomaterials for rapid detection of heavy metal ions. Science China Chemistry, 60 (2017): 329-337.

[12] T. Wadhera, D. Kakkar, G. Wadhwa, Recent advances and progress in development of the field effect transistor biosensor: a review, Journal of Electronic Materials, 48 (2019): 7635-7646.

[13] T. P. Rao, R. Kala, S. Daniel, Metal ion-imprinted polymers-Novel materials for selective recognition of inorganics, Analytica Chimica Acta, 578 (2006): 105-116.

[14] J.Q. Fu, L. X. Chen, Current status and challenges of ion imprinting, Journal of Materials Chemistry A, 3 (2015):13598–13627.

[15] R. Abdeldayem, A preliminary study of heavy metals pollution risk in water, Applied Water Science, 10 (2020):1-4.

[16] R. R. Lauwerys, J. P.Buchet, H.Roels, The relationship between cadmium exposure or body burden and the concentration of cadmium in blood and urine in man. International Archives of Occupational and Environmental Health, 36 (1976):275-285.

[17] K. Sasaki, N. Yongvongsoontorn, K. Tawarada, Y. Ohnishi, T. Arakane, F. Kayama, K. Abe, S. Oguma, N. Ohmura, Cadmium purification and quantification using immunochromatography, Journal of Agricultural and Food Chemistry, 57 (2009):4514-4519.

[18] I. M. Olsson, I. Bensryd, T. Lundh, H. Ottosson, S. Skerfving, A. Oskarsson, Cadmium in blood and urine-impact of sex, age, dietary intake, iron status, and former smoking--association of renal effects, Environmental Health Perspectives, 110 (2003):1185-1190.

[19] A. Navas-Acien, M. Tellez-Plaza, E. Guallar, P. Muntner, E. Silbergeld, B. Jaar, V. Weaver, Blood cadmium and lead and chronic kidney disease in US adults: a joint analysis, American Journal of Epidemiology, 170 (2009): 1156-1164.

[20] L.Björkman, M. Vahter, N. L. Pedersen, Both the Environment and Genes Are Important for Concentrations of Cadmium and Lead in Blood, Environmental Health Perspectives, 108 (2000): 719-722.

[21] Ruth Alison Haggarty, Evaluation of sampling and monitoring designs for water quality, 2012.

[22] World Health Organization (WHO), Environmental Health Criteria 134, 1992.

[23] K. Matyjaszewski, Discovery of the RAFT Process and Its Impact on Radical Polymerization, Macromolecules, 53 (2020):495-497.

[24] M. Sedki , M. Mohamed, M. Fawzy, D. Abdelrehim, M. S. Abdel-Mottaleb, Phytosynthesis of silver–reduced graphene oxide (Ag–RGO) nanocomposite with an enhanced antibacterial effect using Potamogeton pectinatus extract, RSC Advances, 5 (2015):17358-17365.

[25] M. Namvari, C. S. Biswas, M. Galluzzi, Reduced graphene oxide composites with water soluble copolymers having tailored lower critical solution temperatures and unique tube-like structure, Scientific Reports, 7 (2017):44508-44514.

[26] X. Cai, J. Li, Z. Zhang, F. Yang, R. Dong, L. Chen, Novel Pb^{2+} ion imprinted polymers based on ionic interaction via synergy of dual functional monomers for selective solid-phase extraction of Pb^{2+} in Water Samples, ACS Applied Materials & Interfaces, 6 (2014): 305–313.

[27] L. D. Mafu, T. A. M. Msagati, B. B. Mamba, Ion-imprinted polymers for environmental monitoring of inorganic pollutants: synthesis, characterization, and applications, Environmental Science and Pollution Research, 20 (2013):790-802.

[28] A. Kimaro, L. A. Kelly, G. M. Murray, Molecularly imprinted ionically permeable membrane for uranyl ion, Chemical Communications, 14 (2001):1282-1283.

[29] E. Tegou, G.Pseiropoulos, M. K. Filippidou, S. Chatzandroulis, Low-Temperature thermal reduction of graphene oxide films in ambient atmosphere: infra-red spectroscopic studies and gas sensing applications, Microelectronic Engineering, 159 (2016), 146–150.

[30] M. Ciszewski, A. Mianowski, P. Szatkowski, G. Nawrat, J. Adamek, Reduced graphene oxide–bismuth oxide composite as electrode material for supercapacitors. Ionics (Kiel), 21 (2015), 557–563.

[31] A. Paciello, M. G. Santonicola, Supramolecular polycationic hydrogels with high swelling capacity prepared by partial methacrylation of polyethyleneimine, RSC Advances, 5 (2015): 88866-88875.

[32] M. Li, C. Feng, M. Li, Synthesis and characterization of a surface-grafted Cd(II) ion-imprinted polymer for selective separation of Cd(II) ion from aqueous solution, Applied

Surface Science, 332 (2015):463-472.

[33] P. Peng, H. Liu, B. Wu, Q. Tang, Air−stable symmetric ambipolar Field−Effect Transistors based on reduced graphene oxide−OTS self−assembled monolayer heterostructure. ChemNanoMat, 5 (2019): 472-478.

[34] L. Luo, J. S. Jie, W. F. Zhang, Z. B. He, J. X. Wang, G. D. Yuan, Silicon nanowire sensors for Hg(2+) and Cd(2+) ions, Applied Physics letters, 94 (2009):148-150.

[35] P. Bazylewski, S. V. Middelkoop, R. Divigalpitiya, G. Fanchini, Solid-state chemiresistors from two-dimensional MoS_2 nanosheets functionalized with l-Cysteine for in-line sensing of part-per-billion Cd^{2+} ions in drinking water. ACS Omega, 5 (2020): 643-649.

[36] N. Promphet, P. Rattanarat, R. Rangkupan, An electrochemical sensor based on graphene/polyaniline/polystyrene nanoporous fibers modified electrode for simultaneous determination of lead and cadmium. Sensors and Actuators B: Chemical, 207 (2015): 526-534.

[37] M. Lv, X. Wang, J. Li, Cyclodextrin-reduced graphene oxide hybrid nanosheets for the simultaneous determination of lead(II) and cadmium(II) using square wave anodic stripping voltammetry. Electrochimica Acta, 108 (2013): 412-420.

[38] M. Ghanei-Motlagh, M. A. Taher, Novel imprinted polymeric nanoparticles prepared by sol−gel technique for electrochemical detection of toxic cadmium(II) ions, Chemical Engineering Journal, 327 (2017): 135-141.

[39] M. Bakhshpour, A. Denizli, Highly sensitive detection of Cd(II) ions using ion-imprinted surface plasmon resonance sensors, Microchemical Journal, 159 (2020): 105572.

[40] M. Cheng, C. Li, W. Li, Y. Liu, Trace Cd2+ Ions detection on the flower-Like Ag@CuO Substrate. Nanomaterials, 10 (2020): 1664.